

# Facile and Template-Free Method toward Chemical Synthesis of Polyaniline Film/Nanotube Structures

Pei Liu,<sup>1</sup> Yisi Zhu,<sup>2</sup> Jorge Torres,<sup>1</sup> Seung Hee Lee,<sup>3</sup> Minhee Yun<sup>1</sup>

<sup>1</sup>Department of Electrical and Computer Engineering, Swanson School of Engineering, University of Pittsburgh, Pittsburgh, Pennsylvania 15261

<sup>2</sup>Materials Science Division, Argonne National Lab, Lemont, Illinois 60439

<sup>3</sup>Department of BIN Fusion Technology, Chonbuk National University, Jeonju 561-786, Korea

Correspondence to: M. Yun (E-mail: miy16@pitt.edu)

Received 21 April 2017; accepted 24 July 2017; published online 5 September 2017

DOI: 10.1002/pola.28749

**ABSTRACT:** A facile and template-free method is reported to synthesize a new thin film structure: polyaniline (PANI) film/nanotubes (F/N) structure. The PANI F/N is a 100-nm thick PANI film embedded with PANI nanotubes. This well-controlled method requires no surfactant or organic acid as well as relatively low concentration of reagents. Synthesis condition studies reveal that aniline oligomers with certain structures are responsible for guiding the growth of the nanotubes. Electrical characterization also indicates that the PANI F/N possesses similar field-effect transistor characteristics to bare PANI film. With its 20% increased surface-area-to-volume (S/V) ratio

contributed by surface embedded nanotubes and the excellent p-type semiconducting characteristic, PANI F/N shows clear superiority compared with bare PANI film. Such advantages guarantee the PANI F/N a promising future toward the development of ultra-high sensitivity and low-cost biosensors © 2017 Wiley Periodicals, Inc. *J. Polym. Sci., Part A: Polym. Chem.* **2017**, *55*, 3973–3979

**KEYWORDS:** biomaterials; chemical synthesis; conjugated polymers; field-effect transistors; film/nanotubes; nanotube; polyaniline; sensors

**INTRODUCTION** Nanostructured materials have consistently been a popular field of research due to the fact that their high surface-area-to-volume (S/V) ratio can enable plenty of unique physical and chemical properties including high molecular adsorption, large surface tension force, enhanced chemical and biological activities, and large catalytic effects.<sup>1</sup> Polyaniline (PANI), as one of the most studied conductive polymers, is also one of the few polymers that has the capability to adopt numerous different nanoscale shapes. In the past two decades, synthesis and characterizations of different PANI nanostructures such as nanofibers,<sup>2</sup> nanotubes,<sup>3,4</sup> nanospheres,<sup>5</sup> and other fascinating nanostructures<sup>6</sup> have been continuously reported. Among them, PANI nanotubes are undoubtedly favored by many researchers because of their unique one-dimensional (1D) structure, chemical study merits, and excellent electrical properties which may eventually nourish practical application fields such as sensors and field-effect transistors (FETs).<sup>7</sup>

Chemically synthesis of PANI nanotubes is usually achieved by oxidizing aniline in acidic environment. In 1994, Parthasarathy and Martin, for the first time, demonstrated the

synthesis of PANI microtubes using a porous polycarbonate template membrane to guide the growth.<sup>8</sup> These sorts of “hard template” methods were later improved and replaced by the so called “soft template” methods, in which structure directors such as surfactants<sup>9</sup> or organic acid<sup>10</sup> are introduced. Although the soft template methods do not require a post-synthesis template removal process, it is rather difficult to control the morphology and tubular diameter.<sup>11</sup> In 2006, Trchová et al. demonstrated that PANI nanotubes can be synthesized in water with nothing but aniline and ammonium peroxydisulfate (APS).<sup>12</sup> This method limited the number of reagents to two, thus creating a much more simplified chemical reaction model for chemical mechanism study. In this simplified template-free method (STFM), aniline was oxidized and oligomeric products were formed in the first stage of the reaction when the pH is larger than 4. As time went on, the concentration of H<sub>2</sub>SO<sub>4</sub>, the byproduct from the oxidation, increased which brought the pH down below 4. Consequently, the reaction mechanism changed as aniline started to be protonated to anilinium cation, and large molecular weight PANI began to form. It is thought that the nucleated sites on oligomer crystallites were formed with the stack of

Additional Supporting Information may be found in the online version of this article.

© 2017 Wiley Periodicals, Inc.

the phenazine units. Created PANI chains then began to extend from them and continued to form nanotubular structures due to the hydrogen bonding and ionic interactions.<sup>4</sup>

Despite of the study of the PANI nanotube synthesis is mature, the reported nanotubes were mostly nucleated and grew in the bulk solution for mechanism learning purpose, while direct synthesizing nanotubes on substrates were seldom studied.<sup>12</sup> This situation vastly limits the possibility of utilizing PANI nanotubes for device applications given the fact that directly manipulating nanotubes is rather difficult and always requires resource consuming technology such as electron beam lithography. Hence, it is of great interest to develop a facile and low-cost way to make use of the excellent electrical and chemical properties of PANI nanotubes. Interestingly, it is noteworthy that during the late stage of the PANI nanotube synthesis (low pH media), PANI film was always forming on the surface where no “template” existed. This matter of fact provides the possibility to create nanostructures that contain both PANI film and nanotubes. In light of this, herein, we report a facile and template-free method to synthesize a new thin film nanostructure: PANI film/nanotubes, which is a “pizza” like structure that consists of nanoscale thickness PANI film and PANI nanotubes. This method is a variant from the STFM, in which a typical single reaction is replaced with two separate ones. Less concentration of reagents is needed in this method compared with STFM and no surfactant or organic acid is required. The PANI F/N possesses unique surface morphology as well as excellent electrical characteristics. In this work, characterizations were first conducted to assure the successful forming of the nanotubular structures. Different synthesis conditions and a variety of substrates were then attempted for optimization purpose. Finally, a proof-of-concept FET device based on PANI F/N was developed and characterized to demonstrate its potential capability in sensor applications.

## EXPERIMENTAL

### Chemicals and Substrates Preparation

Aniline monomer, perchloric acid (70%), ammonium persulfate (APS)  $((\text{NH}_4)_2\text{S}_2\text{O}_8)$  were purchased from Sigma Aldrich. Polyethylene terephthalate (PET) with thickness of 100  $\mu\text{m}$  was purchased from Goodfellow. Gold substrates were fabricated by depositing 3 nm of Ti followed by 80 nm of Au on a  $\text{SiO}_2/\text{Si}$  wafer using an e-beam evaporator.

### Synthesis Method

PANI F/N was synthesized through a process of two separate reactions as illustrated in Figure 1. Starting pH, as an essential parameter that distinguishes the two reactions, was set as 7 and below 1 for the first (Step A) and second (Step B) reactions, respectively. In the Step A reaction, 0.911 mL of aniline was added into a main beaker with 180 mL DI water and stirred for 30 min to form a uniform mixture in ice bath. Samples which are acting as the substrates for PANI F/N to grow on were cleaned with acetone followed by IPA and three times of DI water. The substrates were then

### Synthesis method

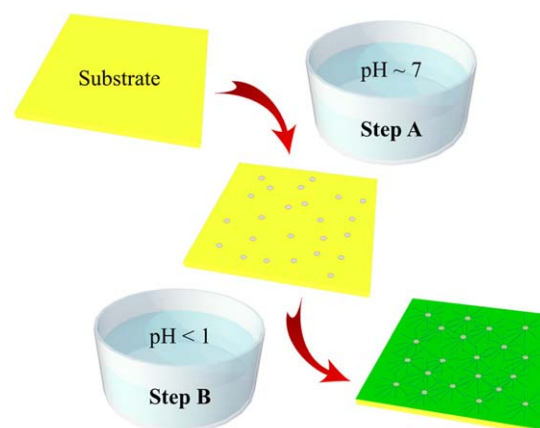


**FIGURE 1** Illustration of the two-step synthesis process. Step A reaction has a starting pH of 7, while the pH in Step B reaction starts below 1. [Color figure can be viewed at [wileyonlinelibrary.com](http://wileyonlinelibrary.com)]

mounted onto a clean wafer, fixed with scotch tapes and immersed in the main beaker. In another beaker, 0.6845g APS was dissolved in 20 mL DI water and put in a freezer to cool down to 0–5 °C. The reaction was initiated by adding the APS solution into the main beaker and the temperature was kept at 0–5 °C under stirring condition (200 rpm). The mixed solution gradually turned brown soon after the initiation. To observe the formation of the PANI nanotubes and investigate how the reaction time in Step A affects the synthesis of PANI nanotubes, different reaction time ranging from 10 min to 4 h was conducted. When the reaction was done, all samples were taken out, rinsed with DI water three times and dried with nitrogen.

To continue the synthesis, a dilute method<sup>13,14</sup> was used which has been demonstrated and commonly used for uniform PANI film synthesis. The preparation of the Step B reaction was similar to the first one. The only difference is that 6 mL of perchloric acid was added into 180 mL of DI water together with aniline monomer to create low pH environment. The reaction was also conducted in ice bath with stirring. Under low pH environment, the mixture solution turned deep dark blue soon after the reaction was initiated which suggests the formation of long chain of PANI. After 4 h, samples were rinsed with DI water, dried with nitrogen, and ready for characterizations.

## RESULTS AND DISCUSSION

### Characterization of PANI Nanotubes

Samples produced through 1 h of Step A reaction and 4 h of Step B reaction were characterized using both scanning electron microscope (SEM) (Quanta 600 FE-SEM) and transmission electron microscope (TEM) (JEOL JEM-2000EX TEM) were utilized. Gold was used as the substrate for synthesizing to achieve better images with SEM due to its excellent conductivity.

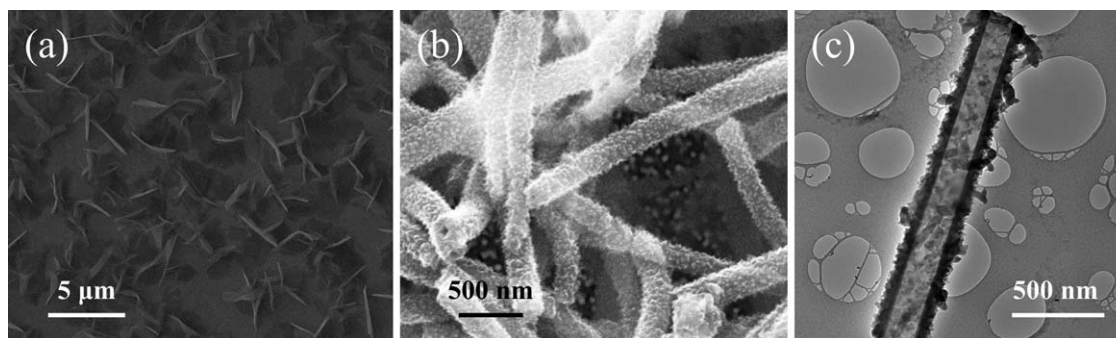


**FIGURE 2** SEM and TEM images of aniline oligomers and PANI nanotubes grown on gold substrate. (a) SEM image of flake-like aniline oligomers formed in Step A. (b) SEM image of PANI nanotubes with a diameter of 300 nm formed after Step B. (c) TEM image of stripped-off PANI nanotube with inner diameter of 200 nm.

Figure 2 shows the characterization results after each reaction. After 1 h of Step A reaction [Fig. 2(a)], flake-like oligomers were first formed on the gold substrate. The grown oligomers are non-conducting, which was confirmed by the obvious surface charging during SEM. After another 4 h of Step B reaction [Fig. 2(b)], clear high-density of cylinder-shaped nanostructures with an average diameter of 300 nm can be found on the substrate. The grown structures show extremely high surface roughness which is attributed to the nanogranular PANI structure formed in the late Step B reaction. In addition, hollow structures can also be observed on the end of some cylinder nanostructures. Further TEM image [Fig. 2(c)] verified the hollow structure with an inner diameter of 200 nm which indicates their nanotubular nature. This result confirms the successful forming of PANI nanotubes. Notably, Step B itself has been well-known and repeatedly demonstrated<sup>15,16</sup> for large molecular weight PANI film synthesis. However, nanotubes were obtained after Step B instead of bare film with the existence of the oligomers formed in nonacidic media. This also proves that the oligomers formed in Step A reaction act as templates for guiding the growth of PANI nanotubes.

To further study the chemical structures of the nanotubes and oligomers, gold samples covered with oligomers prepared in 1 h of Step A (a), nanotubes prepared in 1 h of Step A and 4 h of Step B (b), and PANI film prepared in 4 h of Step B (c) were characterized using Raman spectroscopy (inVia™). The excitation wavelength is 633 nm. As shown in Figure 3, Raman spectrum of PANI film (c) shows peaks at 1590  $\text{cm}^{-1}$  (C=C stretching), 1512  $\text{cm}^{-1}$  (N-H bending), 1470  $\text{cm}^{-1}$  (C=N stretching), 1339  $\text{cm}^{-1}$  (C~N<sup>+</sup> stretching), 1220  $\text{cm}^{-1}$  (C-N stretching), 1165  $\text{cm}^{-1}$  (C-H bending), 810  $\text{cm}^{-1}$  (benzene ring deformation), and 418/525  $\text{cm}^{-1}$  (ring deformation).<sup>17-19</sup> This spectrum matches the typical PANI in emeraldine form.

The synthesized nanotubes (b) show similar Raman spectrum to PANI film (c), which confirms that these are PANI nanotubes. However, peak differences between Raman spectrum (b) and (c) are still observable at 1370  $\text{cm}^{-1}$  and 607  $\text{cm}^{-1}$ . Such differences are believed to be from the

oligomers on nanotubes sample (b) during Step A reaction, which can also be found in the Raman spectrum on oligomers sample (a).<sup>17</sup>

#### Investigation of Synthesis Time in Step A

It is essential to study the condition of PANI nanotube synthesis to gain better understanding of the chemical reactions as well as to optimize the synthesis process. In a typical STFM reaction, one key factor for triggering the growth of PANI nanotubes is the drop of pH due to the byproduct  $\text{H}_2\text{SO}_4$  generated throughout the reaction.<sup>20,21</sup> The reaction can thus transit naturally from “template forming stage” to “PANI synthesis stage” as the time goes on. However, our method deliberately separates those two stages which requires optimizing the synthesis time in Step A reaction while maintaining the same Step B reaction time. To investigate this, a set of experiments were conducted with different synthesis times in Step A reaction (10 min, 30 min, 1 h, 4 h) followed by the same synthesis time in Step B reaction (4 h). Gold was used as the substrate and images were taken with

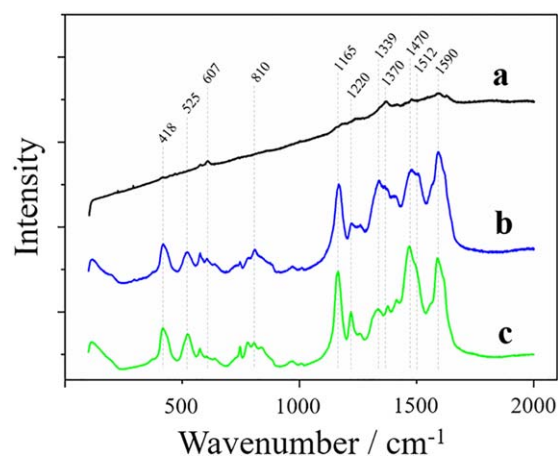


**FIGURE 3** The comparison of Raman spectrums of gold samples with (a) oligomers formed in 1 h of Step A reaction, (b) nanotubes formed in 1 h of Step A reaction followed by 4 h of Step B reaction, (c) PANI film formed in 4 h of Step B reaction. [Color figure can be viewed at wileyonlinelibrary.com]

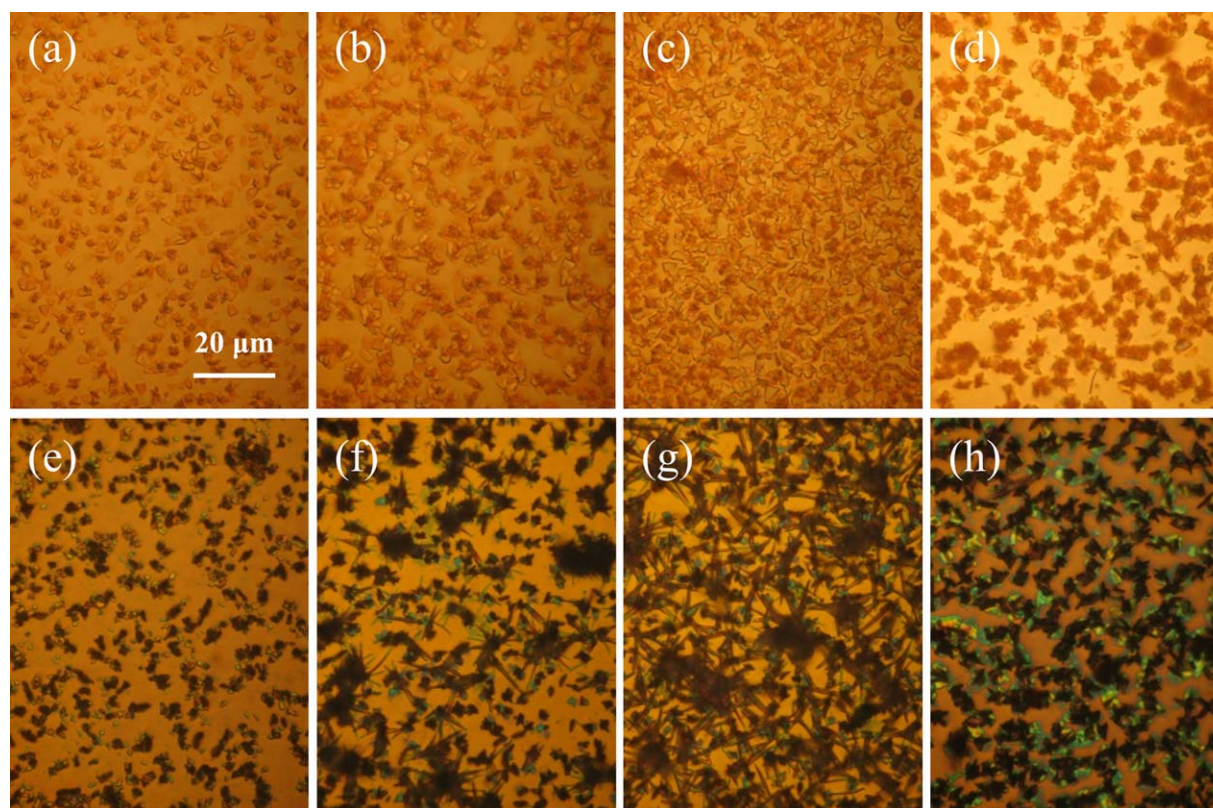


**FIGURE 4** Optical images of synthesis condition optimization results. (a) Ten minutes in Step A. Small flake-like oligomers were formed. (b) Thirty minutes in Step A. The density and size of oligomers were getting larger. Some oligomers started to evolve into clusters. (c) One hour in Step A. The density and size of oligomers kept increasing and reached to maximum. (d) Four hours in Step A. All oligomers existed in the form of clusters. (e) Ten minutes in Step A and 4 h in Step B. No nanotubes sighted. (f) Thirty minutes in Step A and 4 h in Step B. Some nanotube was found. (g) One hour in Step A and 4 h in Step B. High density of nanotubes were observed (h) 4 h in Step A and 4 h in Step B. No nanotube was found. [Color figure can be viewed at [wileyonlinelibrary.com](http://wileyonlinelibrary.com)]

an optical microscope for all samples after each reaction. As shown in Figure 4(a–d), aniline oligomers were formed on the gold surface during Step A. With the increased reaction time, both the density and the average size of the oligomers became larger and larger due to the increased oligomer affinity [from Figs. 4(a) to 3(c)]. In addition, some of the oligomers evolved from a two-dimensional (2D) flake-like structure into a three-dimensional (3D) cluster. However, the oligomers were all turned into the cluster structures after 4 h of Step A process as shown in Figure 4(d). The obvious decrease in oligomer density compared with Figure 4(c) may suggest that a long time in Step A reaction could alter the surface affinity to the oligomer from hydrophilicity to hydrophobicity which eventually caused some of them to detach from the substrate. No change can be observed when the reaction time further increased which is different from a typical STFM. This is because of the utilization of the diluted concentration of both aniline and APS which cannot produce sufficient of  $\text{H}_2\text{SO}_4$  to trigger the PANI synthesis. Figure 4(e–h) shows the results of the four samples after completing another 4 h of Step B. In Figure 4(e), no nanotube can be sighted on the sample with 10 min of Step A and 4 h of Step B reactions. Nanotubes began to form when 30 min of Step

A was used [Fig. 4(f)], and the largest density of nanotubes was achieved after Step B reaction when 1 h of Step A was used [Fig. 4(g)]. It is clear that the nanotubes generated from the oligomers and extended out in every direction. This result agrees with the growing model developed with the STFM.<sup>4</sup> Surprisingly, however, no nanotube was observed on the sample with 4 h in Step A [Fig. 4(h)].

Detailed SEM images of this sample after each reaction were shown in Figure 5. Instead of guiding the growth of PANI

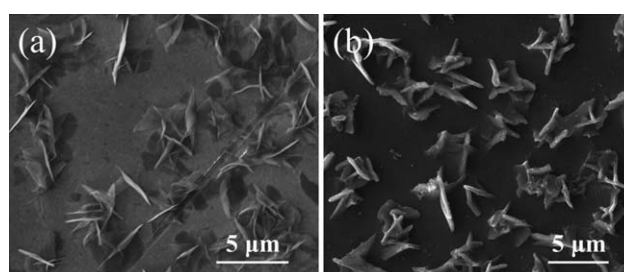


**FIGURE 5** SEM images of the sample with 4 h of Step A before and after Step B. (a) Oligomer clusters before Step B. (b) PANI film covered oligomer clusters after Step B.

nanotubes, the oligomers lost their functions as soft templates, and were covered uniformly by large molecular weight PANI formed in Step B reaction. One possible hypothesis is that the 3D clusters of oligomers formed in nonacidic media for a decent amount of time cannot act as templates for PANI nanotubes to grow on. Therefore, based on these results, we can conclude that the forming of the oligomer templates requires optimal time in Step A reaction, which, in our case, is around 1 h.

### Synthesis of the PANI Film/Nanotubes Structures on Substrates

With the aim of developing PANI F/N for FET device applications, commonly used substrates must be tested. However, it is noteworthy that different surface water affinities may strongly affect the nucleation that occurs on the interface, thus determining the formation of the nanotubes. Therefore, in this work, three commonly used substrates with different water affinities were used. They are PET (hydrophobic), SiO<sub>2</sub> (hydrophilic), and HF-dipped SiO<sub>2</sub> (extremely hydrophilic due to the hydroxyl groups).<sup>22</sup>

A combination of 1 h Step A and 4 h Step B reactions were used for PANI F/N synthesis. To have accurate optical images, transparent PET film was fixed on the holding wafer with the edges sealed so that no reaction would occur on the backside of the film, while the other two substrates were prepared as described in the synthesis method part. All three substrates were characterized by optical microscopy after each reaction. Figure 6(a–c) shows the substrates after only Step A reaction. Flake-like oligomers were observed on all three samples. The densities of the oligomers were similar which were much lower compared with it on gold substrate, and almost no 3D

oligomer was found. However, the oligomers appeared differently according to the substrates: on PET, all of the oligomers were “standing” vertically to the surface; on SiO<sub>2</sub>, half of the oligomers were parallel to the surface with one side facing up; on HF-dipped SiO<sub>2</sub>, all oligomers were parallel to the surface. Figure 6(d–f) shows the three substrates after Step B reaction in addition to Step A.

We observed needle-like nanotubes on both PET and SiO<sub>2</sub> substrates that clearly came from the oligomers. On the contrary, no nanotube was observed on HF-dipped SiO<sub>2</sub> substrate. Instead, a thin PANI film grew directly on top of the oligomers which generated a distinct color difference between Figure 6(c) and Figure 6(f). Similar PANI film covered oligomers can also be seen in Figure 6(e). These results likely suggest that the parallel-to-the-surface-grown oligomers that are attributed to the more hydrophilic substrate surface cannot act as templates for guiding the PANI nanotubes, while the vertically formed ones can. More future chemical studies need to be done to confirm this hypothesis. Notably, the relatively low density of oligomers on PET and SiO<sub>2</sub> substrates created larger space for PANI film to grow on compared with gold substrate, which can also be seen between Figure 6(d) and Figure 6(e) as color difference. This indicates the successful formation of the PANI F/N.

### PANI Film/Nanotubes FET

To further verify the structure as well as the functionality of the PANI F/N, an FET device based on the F/N structure was developed on SiO<sub>2</sub> substrate using the combination of 1 h Step A and 4 h Step B reactions. Detailed description of device fabrication processes can be found in the Supporting Information (S1). An ordinary PANI film based FET device

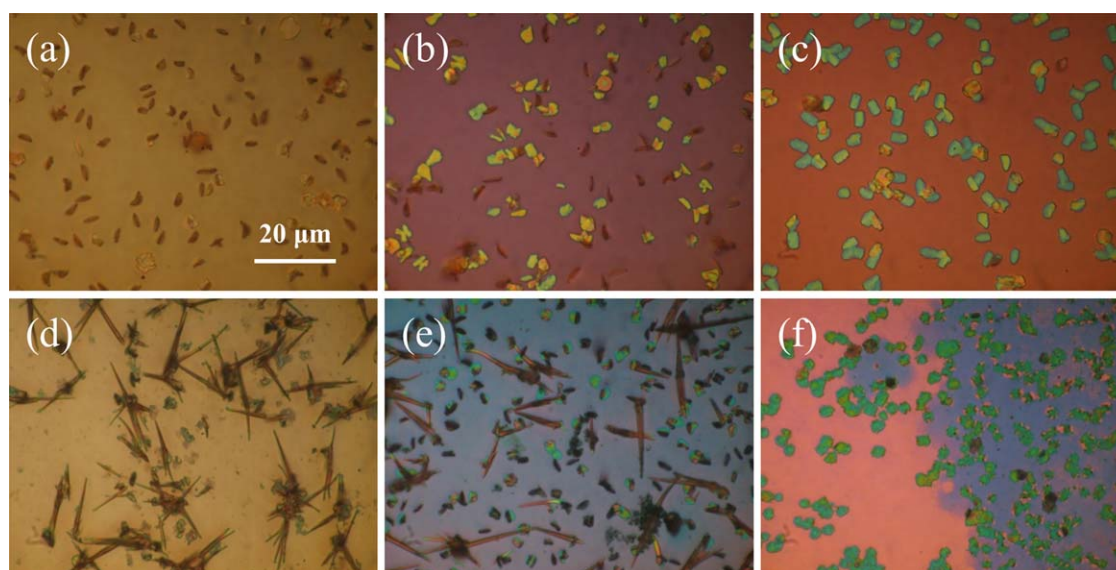


**FIGURE 6** Optical images of PANI film/nanotubes hybrid on various of substrates. (a) PET after Step A, most oligomers grew vertically to the surface. (b) SiO<sub>2</sub> after Step A, half of oligomers were vertical while the other half were parallel to the surface. (c) HF-dipped SiO<sub>2</sub> after Step A, all oligomers were parallel to the surface. (d) PET after Step A and Step B, nanotubes were found. (e) SiO<sub>2</sub> after Step A and Step B, less density of nanotubes was found compared with it on PET. (f) HF-dipped after Step A and Step B, no nanotube was found. [Color figure can be viewed at [wileyonlinelibrary.com](http://wileyonlinelibrary.com)]

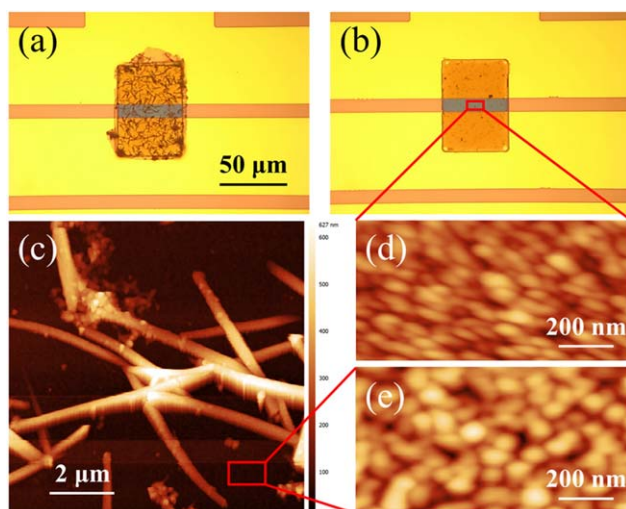


**FIGURE 7** Optical and AFM images of PANI film/nanotubes hybrid FET and bare film FET. (a) Hybrid FET. (b) Bare film FET. (c) Surface topography of the hybrid. (d) High magnification of bare film surface measured by AFM. (e) High magnification of the dark area in (c). [Color figure can be viewed at [wileyonlinelibrary.com](http://wileyonlinelibrary.com)]

was also made and the film was synthesized together with the F/N in Step B reaction. Figure 7(a,b) shows the optical microscope images of both F/N [Fig. 7(a)] and bare film [Fig. 7(b)] FETs. Clearly, despite being covered uniformly with nanotubes, the F/N presents the same color as the film, which not only confirms the existence of PANI film in the F/N structure but also suggests that they have similar thickness and oxidation state.

Further surface topological results measured by atomic force microscope (AFM) (Solver Next AFM) on both FETs are shown in Figure 7(c–e). The nanotubes that grew along the surface have an average diameter around 300–400 nm. Due to some overlapping, the highest point detected is 627 nm from the film surface. This value is within the nanometer scale, which implies that the PANI F/N as a whole is still technically a thin film structure. In addition, high magnification topological results of the film area on F/N [Fig. 7(e)] and bare film [Fig. 7(d)] reveal that they have the same nanogranular surface. Therefore, we confirmed that, structure-wise, the F/N in this study is a thin film structure that consists of ordinary PANI film and PANI nanotubes.

Electrical characterization of both FETs was performed using a typical electrolyte-gate configuration.<sup>23,24</sup> As shown in Figure 7(a,b), the rectangular patterns have a size of 50  $\mu\text{m}$  by 100  $\mu\text{m}$  with a thickness around 100 nm. They are located across the drain and source electrodes with a 10  $\mu\text{m}$  gap in between, while the gate electrode is located near the source. Phosphate-buffered saline solution (0.1X) was dropped onto the FETs and the drain current ( $I_d$ ) versus gate voltage ( $V_g$ ) characteristics as the function of different drain voltages ( $V_d$ ) were obtained by a probe station (Signatone s-1160) shown in Figure 8.

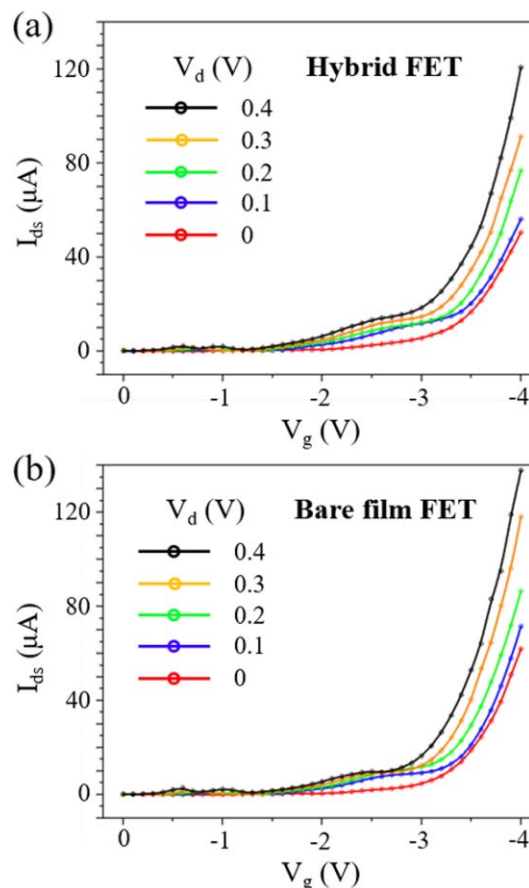


**FIGURE 8** FET characterization of the hybrid FET (a) and bare film FET (b). The  $I_d$ - $V_g$  characteristic was obtained by sweeping  $V_g$  from 0 to  $-4$  V while keeping  $V_d$  staying at different potential level from 0 to 0.4 V. [Color figure can be viewed at [wileyonlinelibrary.com](http://wileyonlinelibrary.com)]

During the measurement,  $V_g$  was constantly decreased from 0 to  $-4$  V while  $V_d$  was fixed at different values ranging from 0 to 0.4 V. Notably, the two FETs have nearly identical characteristics:  $I_{ds}$  increased on decreasing of  $V_g$  due to PANI's p-type nature; The threshold voltage was around  $-1.5$  V after which  $I_{ds}$  started to rise exponentially; as  $V_g$  became more negative than  $-3.5$  V,  $I_{ds}$  became linear. These results indicate that the F/N behaves the same as PANI film formed in the same conditions in terms of surface charge transportation.

One promising application for PANI film/nanotubes is in the development of FET biosensors. A desired design of an FET biosensor requires a semiconductor FET transducer with the ability of being chemically functionalized with bio-receptors such as antibodies and enzymes. When the bio-receptors catch the targets, the charged target molecules start to gate the transducer, thus causing measurable current changes. PANI, as a p-type semiconductor, is capable of being directly functionalized with the presence of cross-linkers such as glutaraldehyde.<sup>25</sup> Well-controlled 2D PANI layer has been successfully demonstrated in biosensor applications (Supporting Information S2). The high sensitivity is attributed to PANI's

good p-type semiconducting property and high S/V ratio. As an improvement, the F/N structure developed in this work possesses approximately 50.7% increase of the surface area and 20% larger S/V ratio given by the embedded nanotubes (Supporting Information S3), which offers more surface sites for bio-receptors/targets complexes. Undoubtedly, with such superiority, PANI F/N can be the next generation conductive polymer-based thin film toward the design of facile and low-cost point-of-care biosensors.

## CONCLUSIONS

In conclusion, we developed a facile method for PANI film/nanotubes synthesis on substrate by splitting the STFM into two reactions: an oligomer templates synthesis reaction (Step A) and a PANI synthesis reaction (Step B). This template-free method requires no organic participant other than aniline as well as less concentration of the reagents. The successful formation of the PANI nanotubes was confirmed by both SEM and TEM, and oligomers that formed in Step A were proved to serve as templates. The reaction time in Step A reaction was then optimized and PANI F/N was successfully synthesized on commonly used substrates such as SiO<sub>2</sub> and PET. By analyzing the microscope images, a hypothesis was proposed: the fully evolved 3D oligomer clusters generated in nonacidic media and parallel-grown flake-like oligomers due to the hydrophilic substrate cannot act as templates for PANI nanotubes to grow on, which requires further in-depth study. Finally, an FET device was developed based on PANI F/N. FET characterization and AFM scanning not only verified the structure of the F/N but also revealed that PANI F/N exhibits excellent p-type semiconductor property similar to the ordinary PANI film while at the same time possesses 50.7% larger surface area. This superiority promises the PANI F/N a great potential in future sensor researches and makes it an ideal substitute of PANI film in thin film related applications.

## ACKNOWLEDGMENT

The authors are grateful to the National Science Foundation (NSF) for the financial support (NSF CBET 1706620) for this research.

## REFERENCES

- 1 E. Roduner, *Chem. Soc. Rev.* **2006**, *35*, 583.
- 2 J. Huang, S. Virji, B. H. Weiller, R. B. Kaner, *J. Am. Chem. Soc.* **2003**, *125*, 314.
- 3 H. Qiu, M. Wan, B. Matthews, L. Dai, *Macromolecules* **2001**, *34*, 675.
- 4 J. Stejskal, I. Sapurina, M. Trchová, E. N. Konyushenko, P. Holler, *Polymer* **2006**, *47*, 8253.
- 5 E. C. Venancio, P. C. Wang, A. G. MacDiarmid, *Synth. Met.* **2006**, *156*, 357.
- 6 J. Stejskal, I. Sapurina, M. Trchová, *Prog. Polym. Sci.* **2010**, *35*, 1420.
- 7 A. N. Aleshin, *Adv. Mater.* **2006**, *18*, 17.
- 8 R. V. Parthasarathy, C. R. Martin, *Chem. Mater.* **1994**, *6*, 1627.
- 9 X. Zhang, S. K. Manohar, *Chem. Commun.* **2004**, *20*, 2360.
- 10 S. K. Pillalamarri, F. D. Blum, A. T. Tokuhiko, J. G. Story, M. F. Bertino, *Chem. Mater.* **2005**, *17*, 227.
- 11 H. Ding, J. Shen, M. Wan, Z. Chen, *Macromol. Chem. Phys.* **2008**, *209*, 864.
- 12 M. Trchová, I. Šeděnková, E. N. Konyushenko, J. Stejskal, P. Holler, G. Čirić-Marjanović, *J. Phys. Chem. B* **2006**, *110*, 9461.
- 13 N. R. Chiou, C. Lu, J. Guan, L. J. Lee, A. J. Epstein, *Nat. Nanotechnol.* **2007**, *2*, 354.
- 14 J. Xu, K. Wang, S. Z. Zu, B. H. Han, Z. Wei, *ACS Nano* **2010**, *4*, 5019.
- 15 P. Liu, J. Huang, D. V. Sanchez, D. Schwartzman, S. H. Lee, M. Yun, *Sens. Actuators B* **2016**, *230*, 184.
- 16 P. Liu, Y. Zhu, S. H. Lee, M. Yun, *Biomed. Microdevices* **2016**, *18*, 113.
- 17 M. Trchová, Z. Morávková, M. Bláha, J. Stejskal, *Electrochim. Acta* **2014**, *122*, 28.
- 18 Z. Rozlívková, M. Trchová, I. Šeděnková, M. Špírková, J. Stejskal, *Thin Solid Films* **2011**, *519*, 5933.
- 19 E. Tomšík, Z. Morávková, J. Stejskal, M. Trchová, J. Zemek, *Synth. Met.* **2012**, *162*, 2401.
- 20 Z. D. Zujovic, J. B. Metson, *Langmuir* **2010**, *27*, 7776.
- 21 E. Konyushenko, M. Trchová, J. Stejskal, I. Sapurina, *Chem. Pap.* **2010**, *64*, 56.
- 22 J. K. Kang, C. B. Musgrave, *J. Chem. Phys.* **2002**, *116*, 275.
- 23 A. S. Dhoot, J. D. Yuen, M. Heeney, I. McCulloch, D. Moses, A. J. Heeger, *Proc. Natl. Acad. Sci. USA* **2006**, *103*, 11834.
- 24 M. M. Alam, J. Wang, Y. Guo, S. P. Lee, H. R. Tseng, *J. Phys. Chem. B* **2005**, *109*, 12777.
- 25 V. V. R. Sai, S. Mahajan, A. Q. Contractor, S. Mukherji, *Anal. Chem.* **2006**, *78*, 8368.